

Wide Image Geometric Mosaic and Measure Algorithm of Mobile Mapping System

WU Meng^{1,2}, GAO Yang^{1,2}, GUAN Bin^{1,2}, LI Kui^{1,2}

1. State Key Laboratory of Geo-information Engineering

2. Xi'an Research Institute of Surveying and Mapping

1,2. Xi'an, China

wumeng19nudit@163.com

Abstract—A wide image mosaic and measure algorithm of mobile mapping system (MMS) has been proposed in this paper. Through constructing the cylindrical panorama projection relationship of triple original digital measurable images (DMIs), the wide image has been mosaiced directly. The corresponding relationship between wide image and object space coordinate has been constructed by utilizing back projection relationship between wide image and original DMIs, and synchro or asynchro stereo DMI pair of the triple original DMIs. Then, the wide image object measure algorithm has been realized. The wide image experiment illustrates that, the method of utilizing cylindrical panorama projection to acquire wide image can be applied in mosaic of sequential wide images in MMS. When original DMI possesses synchro stereo DMI pair, the absolute precision of wide image measure result can be better than 1m and the relative precision of wide image measure result can be better than 0.2m. This accuracy contents with the precision requirement of real vision object measure in city environment.

Keywords—Mobile Mapping System (MMS); Digital Measurable Image (DMI); wide image; cylindrical panorama projection; image mosaic; image measure

I. INTRODUCTION

Mobile Mapping System (MMS) has already been widely used in aspects of military and civil foundational geographic information collection, rapid mapping and platform service nowadays [1-4]. Sensors like global positioning system (GPS), charge coupled device (CCD), inertial navigation system (INS)/dead Reckoning (DR) are usually equipped on MMS vehicles so that road and either sides' land objects can be rapidly shot as Digital Measurable Image(DMI) in speed of 40-80km/h. The accessory files of these DMIs include position and gesture elements of exterior orientation which are needed in photogrammetry analysis. Each DMI pair is marked with its exact sample time. The stereo DMI pairs can be constructed with support of rigor photogrammetry calibration parameters. Various measure method, seamless data fusion and measure-at-anytime-in-need [5] can be realized.

The LYNX of Optech Company, VMX-250 of RIEGL, IP-S2 of Topcon, MX8 of Trimble, StreetMapper of IGI and Street View vehicle of Google are main MMS products in recent years. In China, the Wuhan University, Leader Company, Capital Normal University, Shandong University of

Science and Technology, China Acedemy of Surveying and Mapping, China Acedemy of Sciences in Shenzhen and many research organizations have rolled out their MMS [6].

According to different application aims, sensors of MMS that sample DMIs may either be Ladybug panorama CCDs or be single/double/multi CCD(s) to realize information collection and certain object's measure [7,8]. Considering that exterior orientation elements of these CCDs have been calibrated [9] and are of high imaging resolutions, the captured DMIs can not only be used for user browsing but also be applied for point /line/area measure in DMI.

In this paper, part panorama (or wide image) measure has been researched. Through geometric mosaic processing, measure functions of wide images has been realized. Experiments verified the feasibility and accuracy of the method introduced in this paper. MMS used in this paper was produced by Leader Company in Wuhan, China, as shown in Fig.1. Installing positions of 7 CCDs are shown in Fig.1. Among the 7 CCDs, CCD No.1 and No.2 shoot at the same time as synchro stereo DMI pair, CCD No.3 and No.4 capture simultaneously as synchro stereo DMI pair, CCD No.5 and No.3 have been installed beside CCD No.1 with angles of $\pm 50^\circ$. Triple DMIs captured by CCD No.5, No.1 and No.3 synchronously can be mosiaced into a wide image of a viewing angle more than 150° . CCD No.6 and No.7 are used for both sides and rear street view collection. The wide image geometrically mosaiced from triple DMIs shot by CCD No.5, No.1 and No.3 simultaneously has been mainly discussed in this paper, and object measure algorithms have been implemeted in the experiments.

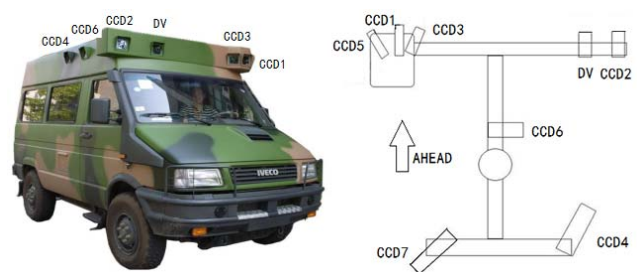


Fig. 1. Ways to Install 7 CCDs in MMS

Researchers have discussed on models like Ladybug panorama, sphere, fisheye, cubes, cylindrical panorama projection and different measure algorithms in mass [10-12]. On the MMS platform used in this paper, the triple DMIs can be mosaiced through partly panoramic cylinders projection. After the cylindrical projection, the geometric relationship can be constructed between wide image coordinate and object space coordinate, so that image mosaic can be well realized just by geometric deformation projection. Object space coordinates in originate DMI captured by CCD No.1 can be obtained by utilizing the synchro stereo relationship between CCD No.1 and No.3. Similarly, Object space coordinates in originate DMI captured by CCD No.1 can be obtained by utilizing the synchro stereo relationship between CCD No.2 and No.4. However, object space coordinates in originate DMI captured by CCD No.5 can be obtained by using the asynchro stereo relationship of CCD No.5. Then object measure can be achieved through geometric tranform from 3 DMIs to wide image.

II. WIDE IMAGE OBTAINING AND GEOMETRIC MOSAIC

A. Features of Panorama Projection

The wide image referred in this paper is part panorama image obtained by cylindrical panorama projection principle. Common panorama projection principles include spherical projection, cubes projection and cylindrical projection. The spherical projection is suitable for observing in 3 degrees of freedom, but it refers to nonlinear deformation in X and Y directions and the data structure for storing the full view image is relatively complex. The cubes panorama image is easy for computer accessing and control, but it should be constructed by images after 90° plane projection, or else the image would deform seriously. Cylindrical projection transforming relationship is relatively simpler and with smaller deformation, and it possesses the feature of no deformation in vertical direction. Therefore, cylindrical panorama is proper for realizing horizontal 360° observing and is convenient for computer storage [13]. In this paper, the geometric relationship has been constructed by part cylindrical panorama projection in MMS experiment platform of Fig.1.

B. Projection and Geometric Mosaic of Cylindrical Wide Image

According to the calibration parameters of all CCD cameras beforehand, the focal length of CCD No.1 is 1276.56 of physical unit. The physical unit should be conversed into pixel unit in convenient for image projection caculation. As shown in Fig.2, if the width and height of the original DMI is W and

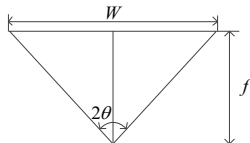


Fig. 2. Relationship between Camera's Pixel Focal Length and Width of Wide Image

H (pixel), the half horizontal viewing angle of the camera is θ , the focal length of the camera is f . Then the horizontal viewing angle 2θ will decide the approximate viewing angle of the wide image which is mosaiced from original triple DMIs. Fig.3 presents the cylindrical front projection relationship and

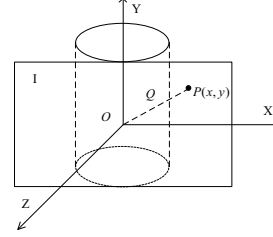


Fig. 3. Cylindrical Front Projection

the $\pm 50^\circ$ installing included angles are known, hence the wide image viewing angle is 150° approximately, and the f can be estimated in unit of pixel as

$$2\theta = 150^\circ / 3, f = W / (2 \tan \theta). \quad (1)$$

Then a point $p(x, y, z)$ in original DMI will be $p(x - W/2, y - H/2, -f)$ when it is in camera coordinate system $p(x_c, y_c, z_c)$. If point Q is the corresponding point of point p after cylindrical projection. As shown in Fig.3, the middle point of the cylinder is the base point of the camera coordinate system, the focal length f is the cylinder radius. When extending the cylinder surface into a flat plane, the relationship between $Q(x', y')$ and $p(x, y)$ can be derived as

$$\begin{cases} x' = f \arctan(-(x - W/2) / f) + f \arctan(W / 2f) \\ y' = f(y - H/2) / \sqrt{(x - W/2)^2 + f^2} + H/2 \end{cases} \quad (2)$$

Fig.4 shows the triple DMIs synchronically captured by CCD No.5, No.1, and No.3 in some typical position. Apparently, the three DMIs have different brightness for the sunlight difference. After cylindrical projection, the width and height of the original DMIs have changed, the image width after cylindrical projection is $W' = 2f\theta$. Through analysing the y' in (2), we can see that y' is the image height after projection. When $x = 0$ or $x = W$, y' has the minimum value, while when $x = W/2$, y' has the maximum value. It means that image width after projection has diminished, and the image height has changed from the minimum to maximum and to minimum again. Fig.5 shows the cylindrical projection transformation result of the three original DMIs in Fig.4. In addition, as the three CCD camera was installed in fixed positions, after the three original DMIs projected to the same cylinder surface, automatic mosaic can be achieved by setting offset values. Fig.6 shows the wide image after just setting proper offset values and cutting the four borders of the mosaic result. As shown in Fig.6, the mosaic result is ideal on



Fig. 4. Three Original DMIs



Fig. 5. Cylindrical Projection of Fig.4



Fig. 6. Mosaic Result

conditions of ignoring the sunlight difference and color uniforming problem of the seam. In this experiment, all sequential DMIs captured by CCD No.5, No.1, and No.3 have been mosaiced using the same parameters, the mosaic results is in a consistently ideal level.

C. Back Projection of Wide Image

The above section illustrates the geometric projection from three original DMIs to wide image. It is the forward process when obtaining a wide image by projection and mosaic. As the pixels in original DMIs are closely linked with elements of exterior and inner orientation in MMS platform, and original DMIs are more convenient for coordinate transform and calculation, it is often necessary to derive back from a point coordinates in wide image to the corresponding coordinate in original DMI. The back projection relationship of the wide image is the inverse function of (2) [14]. So a point $Q(x', y')$ in wide image has a relationship with the corresponding point $p(x, y)$ in original DMI as (3).

$$\begin{cases} x = f \cdot g((x' - f \arctan(W/2f)) / f) + f \arctan(W/2f) \\ y = (y' - H/2) \sqrt{(x - W/2)^2 + f^2} / f + H/2 \end{cases} \quad (3)$$

III. MEASURE ALGORITHM OF WIDE IMAGE

Point or lines in objects in the wide image can be measured given the corresponding relationships (2) and (3) between wide image coordinate and original DMI coordinate. In the experiment, through using the synchro stereo relationship both between CCD 1and3 and between CCD 2and4, and utilizing the asynchro stereo relationship of CCD 5, can the object space coordinate in original DMIs captured by CCD 5,1,3 be obtained. Then taking advantage of the geometric transform relationship from 3 DMIs to wide image, can the object measure in wide image be realized. The point measure algorithm is an object measure algorithm in the wide image. The point measure algorithm is the way to obtain the point in object space coordinate which is coresponding to and transformed from the point in wide image. Point measure algorithm is similar to and simpler than line measure algorithm, so only the line measure algorithm will be introduced in Fig.7.

The line measure algorithm aims to measure any single or continuous line segment(s) in wide image, so that the physical actual length of the line segment(s) of certain accuracy range can be obtained. The concrete algorithm flow is as shown in Fig.7.

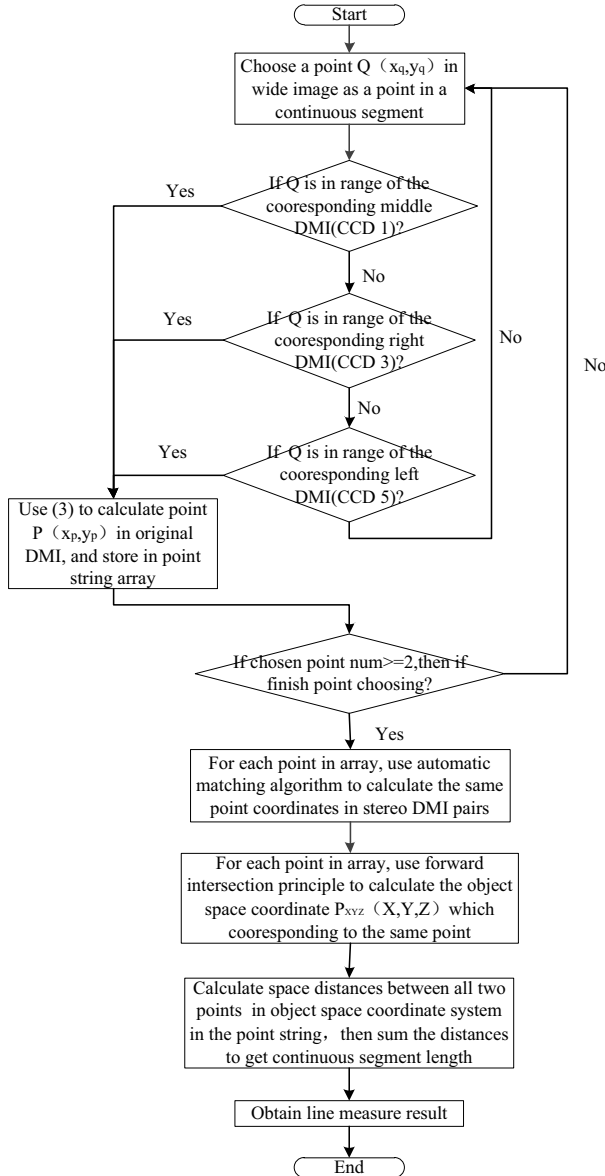


Fig. 7. Line Measure Algorithm FLOW

IV. MEASURE EXPERIMENT

A. Point Measure Experiment

To verify the feasibility and precision of the point measure algorithm in wide image, in this paper 60 marked points have been chosen in intervals of about 10m on a section of quiet road. Points have been marked on sides of the road or on road surface. All points' geodetic coordinates (precision in cm level) have been collected by high precision measuring GNSS (Global Navigation Satellite System) receiver for comparison with point measure results as actual values. MMS experiment platform has been used for collecting sequential DMIs in experiment section of the street. Matlab® has been applied for calculating the transformation process from geometric mosa

and wide image coordinate to object space coordinate. 60 measure results have been calculated in 20 wide images on the left, middle and right sides. Calculation results of the RMS ($\sqrt{\Delta X^2 + \Delta Y^2 + \Delta H^2}$) between measure results and actual coordinate values are as follows in Table 1.

TABLE I. EXPERIMENT RESULT OF POINT MEASURE

Sequential Wide Image No.	Point Measure RMS (m)		
	Left Side	Middle	Right Side
1	1.2668	0.6846	0.8224
2	1.0987	0.5872	0.7726
3	1.1153	0.5385	0.9430
4	1.0016	0.6165	0.8140
5	1.2090	0.6984	0.7252
6	1.4785	0.7304	0.8804
7	1.4141	0.5356	0.8512
8	1.2034	0.6985	0.9627
9	1.1293	0.5830	0.8504
10	1.3437	0.7859	0.9763
11	1.4432	0.7513	0.8964
12	1.0221	0.6171	0.9383
13	1.3709	0.6268	0.8255
14	1.1895	0.6114	0.7401
15	1.4264	0.7204	0.8161
16	1.2879	0.7486	0.6047
17	1.4020	0.6803	0.8307
18	1.3151	0.5171	0.7338
19	1.0193	0.7107	0.8832
20	1.1657	0.6795	0.8244

In Table 1, the absolute precision of point measure in wide image is better than 1.5m. The point measure precision of left side with only asynchro stereo DMIs is better than 1.5m, while the point measure precisions of middle and right sides with synchro stereo DMIs are better than 0.8m and 1.0m.

B. Line Measure Experiment

Similarly, to verify the feasibility and precision of the line measure algorithm in wide image, in this paper 60 marked points also have been chosen in intervals on a section of quiet road. Points have been marked on sides of the road or on road surface. Actual values of all line lengths (precision in mm level) have been collected by soft ruler for comparison with line measure results. MMS experiment platform has been used for collecting sequential DMIs in experiment section of the street. Matlab® has been applied for calculating the line measure process in wide image. 60 line measure results have been calculated in 10 wide images on the left, middle and right sides. Calculation results of the RMS ($\sqrt{\Delta L^2}$) between line measure results and actual line length values are as follows in Table 2.

TABLE II. EXPERIMENT RESULT OF LINE MEASURE

Sequential Wide Image No.	Line Measure RMS (m)		
	Left Side	Middle	Right Side
1	0.4141	0.0865	0.1591
2	0.4451	0.0701	0.1378
3	0.4287	0.0921	0.1910
4	0.2135	0.0523	0.1925
5	0.4612	0.0502	0.1799
6	0.4413	0.0436	0.1305
7	0.2143	0.0913	0.1821

8	0.3790	0.0716	0.1289
9	0.3330	0.0609	0.1712
10	0.4973	0.0688	0.1813
11	0.3250	0.0856	0.1115
12	0.3866	0.0842	0.1167
13	0.2104	0.0678	0.1839
14	0.2830	0.0541	0.1263
15	0.3533	0.0732	0.1544
16	0.3842	0.0833	0.1125
17	0.4236	0.0765	0.1631
18	0.3088	0.0612	0.1423
19	0.4313	0.0723	0.1531
20	0.4786	0.0891	0.1399

In Table 2, the relative precision of line measure in wide image is better than 0.5m. The line measure precision of left side with only asynchro stereo DMIs is better than 0.5m, while the line measure precisions of middle and right sides with synchro stereo DMIs are better than 0.1m and 0.2m.

C. Experiment Result Analysis

As shown in Table 1 and Table 2, objects in the middle DMIs with synchro stereo DMIs have the average minimum error. Objects in right side DMIs with synchro stereo DMIs have average relative bigger error than objects in middle for the influence of shoot angle. Objects in left side DMIs calculated with only asynchro stereo DMIs have often been influenced by base line error which lies in MMS GPS positioning error. Objects in left side DMIs have the average maximum error and cannot satisfy the relative precision requirement of line measure. It is considered that the measure precision is generally used for describing the close-range objects less than 40m in DMIs of MMS [15]. Therefore, the original DMIs should possess synchro stereo DMIs so that could the object measure precision in wide image keep in a consistently better level. Except for the measure errors in synchro stereo DMIs, the new-brought-in error sources and error properties have been analysed in Table 3. In addition, in the experiment process, back projection and the same points chosen artificially have brought in errors fairly the same.

TABLE III. ERROR ANALYSIS OF WIDE IMAGE MEASURE

No.	Error Sources	Error Properties
1	Obtain image point coordinates in original DMI through back projection	Pixel points choosing and geometric deformation in back projection bring in errors.
2	Calculate object space coordinates by the same points in asynchro stereo DMI pairs	GPS positioning error has influenced baseline precision. The position precision of DGPS in MMS is in dm level.

V. CONCLUSIONS

This paper has researched on the object measure method in wide image which was mosaiced from DMIs collected by MMS platform. The geometric relationship between original DMI and wide image, projection algorithm and geometric mosaic method have been studied. The corresponding relationships of pixel points in projection and back projection between original DMI and wide image have been introduced.

The point and line object measure algorithms have been designed and performed in wide images. Experiment results illustrate that the method of obtaining wide image through cylindrical panorama projection and geometric mosaic can be applied in sequential DMIs of MMS platform. On condition that synchro stereo DMIs possess original DMIs, the relative precision of wide image measure is better than 0.2m. This accuracy contents with the requirement for real vision object measure in city environment. A CCD camera is suggested to be added in MMS platform to construct synchro stereo relationship with CCD No.5 in order to keep consistent accuracy when measuring object in a whole wide image.

REFERENCES

- [1] Y. Wang, J. Du, X. Cheng, Z. Liu, K. Lin, "Degradation and encryption for outsourced PNG images in cloud storage," International Journal of Grid and Utility Computing, vol.7, pp.22-28, January 2016.
- [2] S.K.A. Khalid, M. M. Deris, K. M. Mohamad, "Anti-cropping digital image watermarking using Sudoku," International Journal of Grid and Utility Computing, vol. 4, pp.169-177, February 2013.
- [3] D. Martins, H. Guyennet. "Security in wireless sensor networks: a survey of attacks and countermeasures," International Journal of Space-Based and Situated Computing , vol. 1, No. 2/3, 2011.
- [4] A. P. Sabzevar, J. P. Sousa. "Authentication, authorisation and auditing for ubiquitous computing: a survey and vision," International Journal of Space-Based and Situated Computing, vol. 1, No. 1, 2011.
- [5] Z. Xiaodong, "Research on high precision position and orientation method based on digital measurable image and GPS/IMU integration," pp.4-5, Zhengzhou China, PLA Information Engineering University, 2013.
- [6] Z. Zhiyong, "Prospect of panoramic mobile measurement system and its application," Bulletin of Surveying and Mapping, pp.79-81, March 2014.
- [7] A. Jaakkola, J. Hyypä, "A low-cost multi-sensoral mobile mapping system and its feasibility for tree measurements," Isprs Journal of Photogrammetry & Remote Sensing, vol.65, pp.514-522, June 2010.
- [8] G. Yang, "Research on vision navigation key technique based on digital measurable image," pp.29-30, Xi'an China, Chang'an University, 2013.
- [9] C. Ellum, N. El-Sheimy, "The calibration of image-based mobile mapping systems," [www.ReserchGate.net/publication/266167886, February 2015].
- [10] Z. Fanyang, Z. Ruofei, S. Yang, R. Miao, "Vehicle panoramic image matching based on epipolar geometry and space forward intersection," Journal of Remote Sensing. vol.18, pp. 1230—1237, June 2014.
- [11] L. Shuai, C. Jun, S. Min, Z. Lingli, "The derivation and application of spherical panoramic epipolar geometry," Journal of Geo-Information Science. vol.17, pp.274-280, March 2015.
- [12] Z. Zongqian, W. Xin, P. Min, "The key measurable algorithm research based on panoramic image of fish-eye lens," Bulletin of Surveying and Mapping, pp. 70-74, January 2015.
- [13] J. Tie, Z. Guibin, S. Ao, "Review of research status on panorama image mosaic," Journal of Chongqing Technology and Business University(Natural Science Edition). vol.29, pp. 61-64, December 2012.
- [14] L.Jianzhong, "Research on cylindrical panorama image generation based on image drawing," pp.63-64, Harbin Engineering University, Harbin China, 2005.
- [15] Ledor Company. "Introduction of mobile mapping system". [www.3snews.net/index.php?a=show&c=index&catid=28&id=16752&m=content, April 2012].